PCCP

PAPER

View Article Online
View Journal | View Issue

Cite this: *Phys. Chem. Chem. Phys.*, 2015, **17**, 26283

A novel phase of beryllium fluoride at high pressure†

Maksim S. Rakitin,*[a] Artem R. Oganov,*[abcd] Haiyang Niu,[ce] M. Mahdi Davari Esfahani,[a] Xiang-Feng Zhou,[a] Guang-Rui Qian[a] and Vladimir L. Solozhenko[f]

Received 10th July 2015,
Accepted 13th August 2015

DOI: 10.1039/c5cp04010h

www.rsc.org/pccp

A previously unknown thermodynamically stable high-pressure phase of BeF_2 has been predicted using the evolutionary algorithm USPEX. This phase occurs in the pressure range 18–27 GPa. Its structure has *C*2/*c* space group symmetry and contains 18 atoms in the primitive unit cell. Given the analogy between BeF_2 and SiO_2, silica phases have been investigated as well, but the new phase has not been observed to be thermodynamically stable for this system. However, it is found to be metastable and to have comparable energy to the known metastable phases of SiO_2, suggesting a possibility of its synthesis.

I. Introduction

Beryllium fluoride has many applications, such as a coolant component in molten salt nuclear reactors,[1,2] in the production of special glasses[3,4] and in the manufacture of pure beryllium.[5] Structurally, BeF_2 phases are similar to the phases of SiO_2 (Fig. 1): the α-quartz phase of BeF_2 and SiO_2 is stable from 0 to ∼2 GPa, and then transforms into the coesite phase which persists up to ∼8 GPa, and then transforms into stishovite (rutile-type phase) in SiO_2.[6] However, the behavior of BeF_2 experimentally is not known for pressures above 8 GPa (see Scheme 1 in ref. 7).

One of our goals in the present paper is to reveal which phase transitions can occur at higher pressures in BeF_2. Beryllium compounds are extremely toxic for humans, and this limits their experimentation. Computer simulation is a safe and cheap alternative to investigate such structures. In a recent *ab initio* study,[8] the authors explored 13 well-known AB_2 structure types for their possible stability for BeF_2: α-quartz-type ($P3_121$), β-quartz-type ($P6_222$), α-cristobalite-type ($P4_12_12$), β-cristobalite-type ($Fd\bar{3}m$), cubic CaF_2-type ($Fm\bar{3}m$), α-$PbCl_2$-type

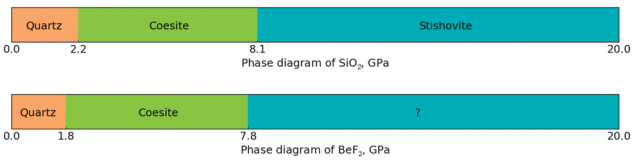

Fig. 1 Phase diagrams of SiO_2[6] and BeF_2[7] at low (up to room) temperatures.

(*Pnma*), Ni_2In-type ($P6_3/mmc$), coesite-type ($C2/c$), rutile-type ($P4_2/mnm$), baddeleyite-type ($P2_1/c$), α-PbO_2-type (*Pbcn*), α-$CaCl_2$-type (*Pnnm*) and pyrite-type ($Pa\bar{3}$) structures. They found that the sequence of pressure-induced phase transitions of BeF_2 up to 50 GPa is as follows: α-quartz-type $\xrightarrow{0.59\,\mathrm{GPa}}$ coesite-type $\xrightarrow{6.47\,\mathrm{GPa}}$ rutile-type $\xrightarrow{24.94\,\mathrm{GPa}}$ α-PbO_2-type structures. Although BeF_2 under pressure has been theoretically investigated by Yu *et al.*,[8] we revisit these results to check for previously unknown structure(s), and we explore the relevance of these findings for SiO_2. Moreover, recently there has been renewed interest on the phase diagram of other related fluoride (CaF_2, SrF_2, and BaF_2) and oxide (UO_2) materials[9,10] under high-*P* and high-*T* conditions, and our results may be relevant to the possibility of new superionic phases.

II. Computational details

Computer simulations of BeF_2 and SiO_2 have been performed in two steps: (1) prediction of a new structure of BeF_2 using the USPEX evolutionary algorithm; (2) calculation of the properties of BeF_2 and SiO_2 in the wide range of pressures from 0 to 50 GPa with a 1 GPa step using DFT.

To find stable lowest-energy crystal structures, we performed a fixed-composition search for the BeF_2 system at different

[a] *Department of Geosciences, State University of New York, Stony Brook, NY 11794, USA. E-mail: maksim.rakitin@stonybrook.edu, artem.oganov@stonybrook.edu*
[b] *Skolkovo Institute of Science and Technology, Skolkovo Innovation Center, Bldg. 3, Moscow 143026, Russia*
[c] *Moscow Institution of Physics and Technology, 9 Institutskiy Lane, Dolgoprudny City, Moscow Region 141700, Russia*
[d] *School of Materials Science, Northwestern Polytechnical University, Xi'an 710072, China*
[e] *Shenyang National Laboratory for Materials Science, Institute of Metal Research, Chinese Academy of Sciences, Shenyang 110016, China*
[f] *LSPM-CNRS, Université Paris Nord, 93430 Villetaneuse, France*

† Electronic supplementary information (ESI) available: CIF file of the BeF_2 *C*2/*c* structure at 20 GPa. See DOI: 10.1039/c5cp04010h

pressures (15, 20 and 25 GPa) using the USPEX code,[11–13] in conjunction with first-principles structure relaxations using density functional theory (DFT) within the Perdew–Burke–Ernzerhof (PBE) generalized gradient approximation (GGA),[14] as implemented in the VASP package.[15] We employed projector augmented wave (PAW)[16] potentials with 2 valence electrons for Be and 7 for F. The wave functions were expanded in a plane-wave basis set with a kinetic energy cutoff of 600 eV and Γ-centered meshes for Brillouin zone sampling with a reciprocal space resolution of $2\pi \times 0.10$ Å^{-1}.

We used the VASP package to carefully reoptimize the obtained structures before calculating phonons, elasticity, electronic density of states (DOS), and hardness of BeF_2 and SiO_2. For these relaxations, we also used a plane-wave cutoff of 600 eV and k-meshes with a resolution of 0.10 Å^{-1}. Phonon calculations have been performed using Phonopy[17] and Quantum Espresso[18] codes for the relaxed structures at pressures where these structures are found to be thermodynamically stable. Hardness was calculated using 3 methods: the Lyakhov–Oganov model[19] based on the strength of bonds between atoms and the bond network topology, the Chen–Niu model[20] which uses elastic constants obtained from DFT calculations and the Mukhanov–Kurakevych–Solozhenko thermodynamic model of hardness.[21]

III. Results and discussion

USPEX allowed us to find a new structure of BeF_2, stable at 18–27 GPa (Fig. 2). The structure has a $C2/c$ space group and contains 12 formula units in the Bravais cell (6 in the primitive cell) with a = 8.742 Å, b = 8.695 Å, c = 4.178 Å and β = 66.1° (at 20 GPa). The calculated density of this new $C2/c$ phase is 4.2% higher than the density of the coesite phase, both at 20 GPa. For reference, here are lattice parameters for BeF_2–stishovite at 30 GPa: $a = b$ = 3.986 Å, c = 2.501 Å and $\alpha = \beta = \gamma = 90°$. The value of the bulk modulus B_0 = 22.7 GPa of the $C2/c$ structure of BeF_2 with its pressure derivative $B_0' = 3.9$ was obtained from a least-squares fit using the Murnaghan equation of state[22] (Fig. 3). The zero-pressure unit cell volume was taken as V_0 = 213.7 Å^3.

A. Thermodynamic stability

We have calculated the enthalpies of α-quartz ($P3_221$), coesite ($C2/c$), coesite-II ($C2/c$), stishovite ($P4_2/mnm$), and α-PbO_2-type ($Pbcn$) structures and our new structure ($C2/c$) for both BeF_2 and

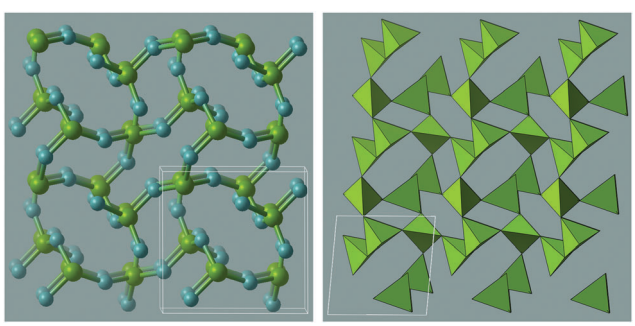

Fig. 2 $C2/c$ structure of BeF_2, stable at 18–27 GPa.

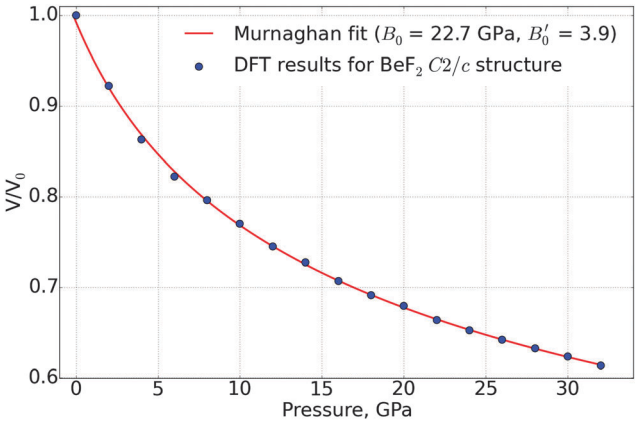

Fig. 3 Equation of state of the BeF_2 $C2/c$ structure.

SiO_2 at different pressures from 0 to 50 GPa with a 1 GPa step. The results are presented in Fig. 4.

1. BeF_2 under pressure. For the case of BeF_2 the α-quartz structure is stable from 0 to 4 GPa, followed by the coesite structure stable from 4 to 18 GPa, and the $C2/c$ structure is found to be stable between 18 and 27 GPa, which then gives place to the stishovite structure at higher pressures (Fig. 4(a)).

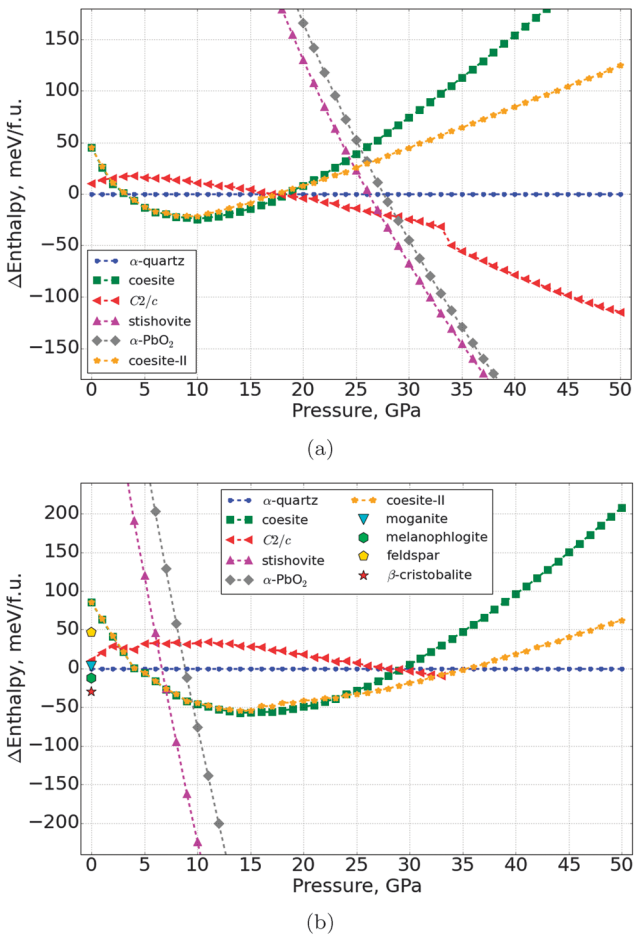

Fig. 4 Enthalpies (relative to α-quartz) of (a) BeF_2 and (b) SiO_2 phases as a function of pressure.

We see transition from the coesite-type to $C2/c$, then to the rutile-type, but at much higher pressure (27 GPa against 6.47 GPa in ref. 8, where LDA was used). According to Demuth *et al.*,[23] the LDA approximation used in ref. 8 underestimates phase transition pressures, whereas using the GGA yields more reliable results. The α-PbO_2-type structure is not stable at any pressure (in the investigated interval from 0 to 50 GPa) for BeF_2 (though it is close to stability at ∼27 GPa), while for SiO_2 it is indeed stable at pressures above ∼80–90 GPa.[24]

2. SiO_2 under pressure. From Fig. 4(b) it is clearly seen that in SiO_2 the transition from α-quartz to coesite occurs at 5 GPa, followed by transformation to stishovite at ∼7 GPa, which continues to be stable up to 50 GPa. This phase transition sequence is in good agreement with experiments[6] and with the GGA results obtained by Demuth *et al.*,[23] Oganov *et al.*[24] and the LDA results of Tsuchiya *et al.*;[25] it is known though[23] that the GGA is more accurate than the LDA for phase transition pressures. The new structure is not stable at any pressure for SiO_2, but at 0 GPa is only 10 meV per f.u. higher in energy than α-quartz, and should be synthesizable as a metastable phase. Typically, kinetic barriers in such covalent tetrahedral phases are very high, *i.e.* metastable phases of such a type exist in nature for millions of years. However, it is quite hard to estimate the magnitude of the barrier both theoretically and experimentally, and this is out of the scope of the present work. Our results of coesite → coesite-II transition are in good agreement with the recent study of Černok *et al.*,[26] where they observe coesite at 20.3 GPa, and after an abrupt change in the diffraction pattern between ∼20 and ∼28 GPa – coesite-II at 27.5 and 30.9 GPa.

3. Metastable structures of SiO_2. It is well known that SiO_2 α-quartz is thermodynamically stable at ambient pressure. However, there are numerous known SiO_2 polymorphs which are metastable, but exist in nature or can be synthesized. We examined SiO_2 feldspar, baddeleyite, melanophlogite and moganite at 0 GPa. El Goresy *et al.*[27] claimed a baddeleyite-like post-stishovite phase of silica in the Shergotty meteorite, however later that controversial phase turned out to be α-PbO_2-like silica.[28] Our calculations confirm that the baddeleyite-like form of SiO_2 is very unfavorable at 0 GPa and spontaneously (barrierlessly) transforms into the α-PbO_2-like structure. We have found that SiO_2–feldspar, moganite and melanophlogite are energetically very close to the stable phase (α-quartz) and to the new $C2/c$ structure. Differences in enthalpy between melanophlogite, the new structure, and α-quartz are less than 20 meV per f.u. (see Fig. 4(b)). The fact that the complex open structure of melanophlogite (138 atoms per cell) has a slightly lower energy than α-quartz can be explained by errors of the GGA, which were discussed in detail by Demuth *et al.*[23] They also found that β-cristobalite (Fig. 4(b)) is lower in energy by about 30 meV per SiO_2 than α-quartz, confirmed by calculations of Zhang *et al.*,[29] showing that the GGA slightly overstabilizes low-density structures.

B. Lattice dynamics

Since the new structure of BeF_2 appears to be thermodynamically stable, analysis of dynamical stability (phonon dispersion) has been performed for this structure as well as for all other structures at pressures where they were found to be thermodynamically stable. Our results show that BeF_2 α-quartz at 0 GPa, coesite at 5 GPa, a new structure at 25 GPa and stishovite at 30 GPa do not have imaginary frequencies. Similar results are observed for SiO_2 α-quartz at 0 GPa, coesite at 5 GPa and stishovite at 10 GPa. Fig. 5 shows dynamical stability of the new structure of BeF_2 since no imaginary frequencies are observed in the phonon dispersion plot.

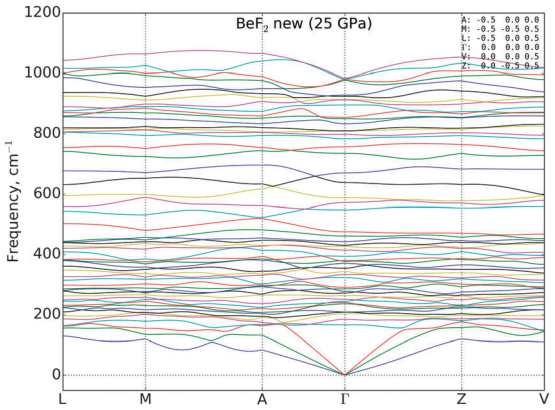

Fig. 5 Phonon dispersion curves showing the dynamical stability of the $C2/c$ structure of BeF_2 at 25 GPa.

C. Electronic properties

According to Fig. 6, all BeF_2 phases are insulators, the DFT band gap increases from ∼7 to ∼10 eV with increasing pressure from 0 to 30 GPa and the value of the gap is in good agreement with the data of Yu *et al.*[8]

For SiO_2 (Fig. 7) we also observe insulating behavior, and the band gap is about 6 eV and remains almost unchanged with increasing pressure.

D. Hardness

Three models have been exploited to calculate hardnesses – the Lyakhov–Oganov,[19] Chen–Niu[20] and Mukhanov–Kurakevych–Solozhenko[21] models. The first approach is based on concepts

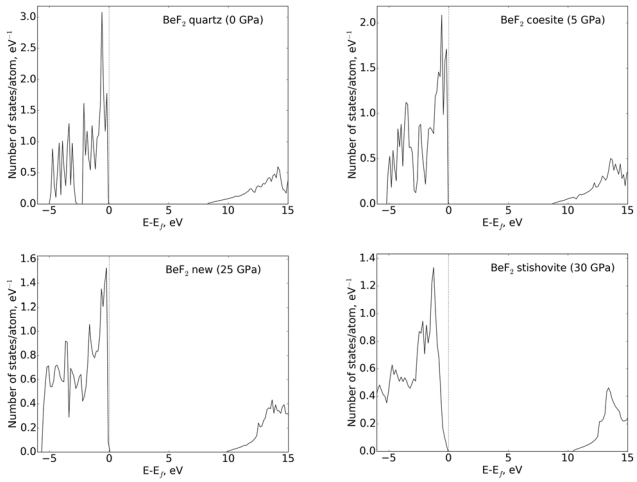

Fig. 6 Density of states of BeF_2 in the α-quartz (at 0 GPa), coesite (at 5 GPa), $C2/c$ structure (at 25 GPa), and stishovite (at 30 GPa) phases.

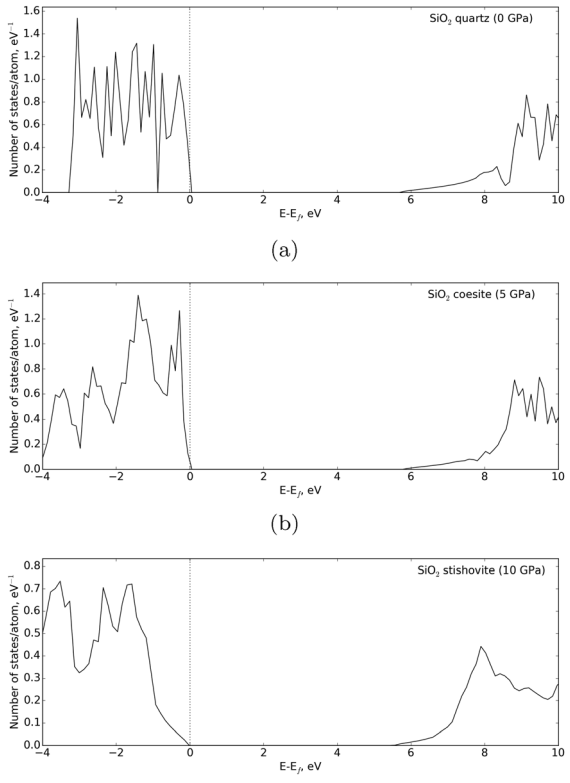

Fig. 7 Density of states of SiO_2 in the (a) α-quartz (at 0 GPa), (b) coesite (at 5 GPa) and (c) stishovite (at 10 GPa) phases.

of bond strengths and bond topology to compute hardness. Detailed description of the methodology can be found in ref. 19. This model has been implemented in the USPEX code, and for greater convenience has also been implemented as an online utility available at http://han.ess.sunysb.edu/hardness/. The second method of hardness calculation is the Chen–Niu model, which is based on elastic tensor components and also implemented in the USPEX code. The third one is a thermodynamic model of hardness.

The results can be seen in Table 1. Experimental data are provided where available – Vickers hardness of SiO_2–quartz,[30] SiO_2–coesite[21] and SiO_2–stishovite.[31] From Table 1 it is clearly seen that the calculated hardness of SiO_2 quartz and stishovite is much higher than the one of BeF_2 analogs. The hardness of BeF_2 and SiO_2 in the new $C2/c$ structure is comparable with the hardness of α-quartz and coesite.

IV. Conclusions

We have examined the thermodynamic, vibrational, electronic and elastic properties of BeF_2 and SiO_2 phases using DFT calculations. The sequence of pressure-induced phase transitions of BeF_2 up to 50 GPa is as follows: α-quartz-type $\xrightarrow{4\,\mathrm{GPa}}$ coesite-type $\xrightarrow{18\,\mathrm{GPa}}$ $C2/c$ $\xrightarrow{27\,\mathrm{GPa}}$ stishovite (rutile-type) structures. We found a new phase of BeF_2 which is thermodynamically stable at pressures from 18 to 27 GPa. This phase is not observed in SiO_2, but could be synthesized in principle. Analysis of electronic properties has shown that BeF_2 and SiO_2 remain insulators in a wide range of pressures (from 0 to 50 GPa). Hardness of BeF_2 and SiO_2 in the new structure is comparable with hardness of α-quartz and coesite at 0 GPa. Hardnesses of metastable SiO_2 structures have been examined as well.

Appendix A: densities of BeF_2 and SiO_2 structures

Table 2 shows densities of BeF_2 structures at 0 and 20 GPa and SiO_2 structures at 0 GPa.

Table 1 Hardness of BeF_2 and SiO_2 structures at 0 GPa in GPa. For the metastable SiO_2 structures we present enthalpies relative to α-quartz (in meV per formula unit)

	BeF_2			SiO_2		
	Lyakhov–Oganov	Chen–Niu	Mukhanov *et al.*[a]	Lyakhov–Oganov	Chen–Niu	Experiment
Quartz	7.1	7.5	11.0	20.0	12.5	12.0[b]
Coesite	8.2	8.3	11.7	22.3	8.4	20.0[b]
New structure	7.3	6.8	13.5	19.1	6.7	—
Stishovite	8.2	12.7	15.1	29.0	28.7	33.0[b]

	Metastable structures (SiO_2 only)		
		Hardness, GPa	
	Relative enthalpy, meV per f.u.	Lyakhov–Oganov model	Chen–Niu model
Feldspar	47	6.7	11.8
Baddeleyite	726	29.6	28.0
Melanophlogite	−13	12.5	3.3
Moganite	3	19.5	12.8

[a] Thermodynamic model of hardness (ref. 21). [b] Vickers hardness.

Table 2 Densities of BeF_2 and SiO_2 structures

System	Number of atoms	Volume, Å^3 per cell	Density, g cm^{-3}
BeF_2 at 0 GPa			
α-Quartz	9	105.167	2.244
Coesite	24	254.636	2.472
Coesite-II	96	1021.960	2.464
*C*2/*c*	18	213.696	2.209
Stishovite	6	47.771	3.294
BeF_2 at 20 GPa			
α-Quartz	9	73.078	3.230
Coesite	24	202.001	3.116
*C*2/*c*	18	145.159	3.252
Stishovite	6	41.492	3.793
SiO_2 at 0 GPa			
α-Quartz	9	116.934	2.580
Coesite	24	283.341	2.839
Coesite-II	96	1137.296	2.830
*C*2/*c*	18	243.569	2.477
Stishovite	6	48.185	4.174
α-PbO_2-type	12	94.623	4.251

Author contributions

M.R., H.N. and M.D. performed the calculations, and M.R. and A.R.O. contributed to the analysis and wrote the paper. X.F.Z and G.R.Q. provided technical assistance with calculations. V.L.S. proposed the idea, performed calculations of hardness and participated in the discussion.

Competing financial interests

The authors declare no competing financial interests.

Acknowledgements

We thank the National Science Foundation (EAR-1114313, DMR-1231586), DARPA (Grant No. W31P4Q1210008), the Government of Russian Federation (grant No. 14.A12.31.0003), and Foreign Talents Introduction and Academic Exchange Program (No. B08040). Also, we thank Dr V. A. Mukhanov for valuable comments.

References

1 C. Weaver, R. Thoma, H. Insley, H. Friedman and U. A. E. Commission, *Phase equilibria in molten salt breeder reactor fuels: the system LiF-BeF_2-UF_4-ThF_4,* Oak Ridge National Laboratory, 1961.
2 O. Beneš and R. Konings, Thermodynamic properties and phase diagrams of fluoride salts for nuclear applications, *J. Fluorine Chem.*, 2009, **130**, 22–29.
3 J. Parker and P. France, in *Glasses and Glass-Ceramics*, Optical properties of halide glasses, ed. M. Lewis, Springer, Netherlands, 1989, pp. 156–202.
4 F. Gan, Optical properties of fluoride glasses: a review, *J. Non-Cryst. Solids*, 1995, **184**, 9–20.
5 H. Hausner, *Beryllium, its metallurgy and properties*, ed. H. H. Hausner, University of California Press, Berkeley, 1965, p. 322.
6 V. Swamy, S. Saxena, B. Sundman and J. Zhang, A thermodynamic assessment of silica phase diagram, *J. Geophys. Res.: Solid Earth*, 1994, **99**, 11787–11794.
7 P. Ghalsasi and P. Ghalsasi, Single crystal X-ray structure of BeF_2: α-quartz, *Inorg. Chem.*, 2011, **50**, 86–89.
8 F. Yu, M. Xu, M. Jiang and J.-X. Sun, The phase transitions and electronic structures of crystalline BeF_2 under high-pressure: first-principle calculations, *Solid State Commun.*, 2013, **169**, 14–19.
9 C. Cazorla and D. Errandonea, High-pressure, high-temperature phase diagram of calcium fluoride from classical atomistic simulations, *J. Phys. Chem. C*, 2013, **117**, 11292–11301.
10 C. Cazorla and D. Errandonea, Superionicity and polymorphism in calcium fluoride at high pressure, *Phys. Rev. Lett.*, 2014, **113**, 235902.
11 A. Oganov and C. Glass, Crystal structure prediction using *ab initio* evolutionary techniques: Principles and applications, *J. Chem. Phys.*, 2006, **124**, 244704.
12 A. Oganov, A. Lyakhov and M. Valle, How evolutionary crystal structure prediction works – and why, *Acc. Chem. Res.*, 2011, **44**, 227–237.
13 A. Lyakhov, A. Oganov, H. Stokes and Q. Zhu, New developments in evolutionary structure prediction algorithm USPEX, *Comput. Phys. Commun.*, 2013, **184**, 1172–1182.
14 J. Perdew, K. Burke and M. Ernzerhof, Generalized gradient approximation made simple, *Phys. Rev. Lett.*, 1996, **77**, 3865–3868.
15 G. Kresse and J. Furthmüller, Efficient iterative schemes for *ab initio* total-energy calculations using a plane-wave basis set, *Phys. Rev. B: Condens. Matter Mater. Phys.*, 1996, **54**, 11169–11186.
16 G. Kresse and D. Joubert, From ultrasoft pseudopotentials to the projector augmented-wave method, *Phys. Rev. B: Condens. Matter Mater. Phys.*, 1999, **59**, 1758–1775.
17 A. Togo, F. Oba and I. Tanaka, First-principles calculations of the ferroelastic transition between rutile-type and $CaCl_2$-type SiO_2 at high pressures, *Phys. Rev. B: Condens. Matter Mater. Phys.*, 2008, **78**, 134106.
18 P. Giannozzi, S. Baroni, N. Bonini, M. Calandra, R. Car, C. Cavazzoni, D. Ceresoli, G. Chiarotti, M. Cococcioni, I. Dabo, A. Corso, S. Gironcoli, S. Fabris, G. Fratesi, R. Gebauer, U. Gerstmann, C. Gougoussis, A. Kokalj, M. Lazzeri, L. Martin-Samos, N. Marzari, F. Mauri, R. Mazzarello, S. Paolini, A. Pasquarello, L. Paulatto, C. Sbraccia, S. Scandolo, G. Sclauzero, A. Seitsonen, A. Smogunov, P. Umari and R. Wentzcovitch, Quantum espresso: a modular and open-source software project for quantum simulations of materials, *J. Phys.: Condens. Matter*, 2009, **21**, 395502.
19 A. Lyakhov and A. Oganov, Evolutionary search for superhard materials: Methodology and applications to forms of carbon and TiO_2, *Phys. Rev. B: Condens. Matter Mater. Phys.*, 2011, **84**, 092103.

20 X.-Q. Chen, H. Niu, D. Li and Y. Li, Modeling hardness of polycrystalline materials and bulk metallic glasses, *Intermetallics*, 2011, **19**, 1275–1281.
21 V. Mukhanov, O. Kurakevych and V. Solozhenko, The interrelation between hardness and compressibility of substances and their structure and thermodynamic properties, *J. Superhard Mater.*, 2008, **30**, 368–378.
22 F. Murnaghan, The compressibility of media under extreme pressures, *Proc. Natl. Acad. Sci. U. S. A.*, 1944, **30**, 244–247.
23 T. Demuth, Y. Jeanvoine, J. Hafner and J. Ángyán, Polymorphism in silica studied in the local density and generalized-gradient approximations, *J. Phys.: Condens. Matter*, 1999, **11**, 3833.
24 A. Oganov, M. Gillan and G. Price, Structural stability of silica at high pressures and temperatures, *Phys. Rev. B: Condens. Matter Mater. Phys.*, 2005, **71**, 064104.
25 T. Tsuchiya, R. Caracas and J. Tsuchiya, First principles determination of the phase boundaries of high-pressure polymorphs of silica, *Geophys. Res. Lett.*, 2004, **31**, 1–4.
26 A. Černok, E. Bykova, T. Ballaran, H.-P. Liermann, M. Hanfland and L. Dubrovinsky, High-pressure crystal chemistry of coesite-I and its transition to coesite-II, *Z. Kristallogr. – Cryst. Mater.*, 2014, **229**, 761–773.
27 A. El Goresy, L. Dubrovinsky, T. Sharp, S. Saxena and M. Chen, A monoclinic post-stishovite polymorph of silica in the Shergotty meteorite, *Science*, 2000, **288**, 1632–1634.
28 L. Dubrovinsky, N. Dubrovinskaia, S. Saxena, F. Tutti, S. Rekhi, T. Bihan, G. Shen and J. Hu, Pressure-induced transformations of cristobalite, *Chem. Phys. Lett.*, 2001, **333**, 264–270.
29 J. Zhang, Q. Zeng, A. Oganov, D. Dong and Y. Liu, High throughput exploration of $Zr_xSi_{1-x}O_2$ dielectrics by evolutionary first-principles approaches, *Phys. Lett. A*, 2014, **378**, 3549–3553.
30 A. Oganov and A. Lyakhov, Towards the theory of hardness of materials, *J. Superhard Mater.*, 2010, **32**, 143–147.
31 J. Léger, J. Haines, M. Schmidt, J. Petitet, A. Pereira and J. da Jornada, Discovery of hardest known oxide, *Nature*, 1996, **383**, 401.

